

---

This is the **accepted version** of the journal article:

Calvo-Lopez, Antonio; Ymbern, Oriol; Puyol Bosch, M. del Mar; [et al.]. «Soluble reactive phosphorous determination in wastewater treatment plants by automatic microanalyzers». *Talanta*, Vol. 221 (January 2021), art. 121508. DOI 10.1016/j.talanta.2020.121508

---

This version is available at <https://ddd.uab.cat/record/288006>

under the terms of the  license

# Soluble reactive phosphorous determination in wastewater treatment plants by automatic microanalyzers

Antonio Calvo-López, Oriol Ymbern, Mar Puyol and Julián Alonso-Chamarro\*

<sup>a</sup>Group of Sensors and Biosensors, Department of Chemistry, Autonomous University of Barcelona, Edifici Cn, 08193 Bellaterra, Barcelona, Spain

\*Corresponding author. E-mail address: [Julian.Alonso@uab.es](mailto:Julian.Alonso@uab.es); Tel: +34935812149

## Abstract

The analysis of soluble reactive phosphate (SRP) in water is key to control water quality. In order to continuously monitor orthophosphate content in water during treatment processes and in the effluents of wastewater treatment plants, conventional procedures, usually performed in a laboratory, must be adapted. This means pursuing efforts on miniaturizing systems to operate in situ and automating analytical methods to work on-line. The design, construction and evaluation of an automatic and low cost cyclic olefin copolymer (COC)-based spectrophotometric microanalyzer, capable of operating in unattended conditions, is presented to monitor soluble reactive phosphorous, as orthophosphate ion, in wastewater samples coming from sewage treatment plants. The microsystem, constructed by CNC micromilling and using a multilayer approach, integrates microfluidics to carry out the phosphomolybdenum blue (PMB) reaction and an optical flow-cell for the spectrophotometric orthophosphate determination in a single polymeric substrate smaller than a credit card. It is connected to a compact optical detection system composed by a LED emitting at 660 nm and a PIN-photodiode, both integrated in a PCB. Flow management is automatically performed by programmed microvalves and micropumps, which control autocalibration processes and allow unattended operation. Analytical features after the optimization of the microfluidic platform and the chemical and the hydrodynamic variables, were a linear range from 0.09 to 32 mg L<sup>-1</sup> P and a detection limit of 0.03 mg L<sup>-1</sup> P with a sampling rate of 24 samples h<sup>-1</sup>, demonstrating the microanalyzer

1 suitability for SRP monitoring in water. Moreover, real samples were analyzed obtaining  
2 promising results.  
3

4 **Keywords:** Lab on a chip, Environment, Miniaturization, Phosphorous, Wastewater, Optical  
5 detection.  
6  
7

## 8 **1. Introduction**

9  
10  
11  
12 Phosphorous is one of the most important parameters to analyze in water quality control of  
13 aquatic ecosystems [1,2]. The special monitoring interest lies on the fact that it is a limiting  
14 nutrient for the growth of some algae, plants and bacteria, so that, an excess of dissolved  
15 phosphorous in water causes the so-called eutrophication [3–5]. This is characterized by an  
16 excessive development of biomass, which means a fast consuming of oxygen present in the  
17 medium causing among others the reduction of diversity, fish death, decreasing water  
18 transparency, taste and odor problems, increasing water treatments costs, interfering of  
19 recreational uses (swimming, boating, fishing, etc.) and the possibility of toxic or inedible algal  
20 blooms. All these facts cause a drastically reduction of water quality and could be a risk for  
21 human health [4,6]. In general, levels above  $0.1 \text{ mg L}^{-1} \text{ P}$  indicates a severe eutrophication [7].  
22 Phosphorus reaches wastewater treatment plants (WWTP) through the influent streams coming  
23 from both domestic and industrial wastewater at concentrations that must be removed for the  
24 protection of the receiving waters. Different phosphorus species, both dissolved and particulate  
25 forms, can be found in aquatic ecosystems. The fraction of soluble reactive phosphorus (SRP),  
26 composed mainly by orthophosphate, provides an estimation of the more readily bioavailable  
27 amount of phosphorus. Typical phosphorous content in municipal wastewater can range from 4-  
28 25  $\text{mg L}^{-1} \text{ P}$ , while legal orthophosphate concentration in discharges of WWTP range from 0.1  
29  $\text{mg L}^{-1} \text{ P}$  in sensitive water bodies to 2  $\text{mg L}^{-1} \text{ P}$  in rivers or sea [7–10]. Thus, monitoring SRP  
30 during the treatment processes and in the effluents of WWTP allows verifying that the amount  
31 of phosphorous will not produce eutrophication in the receiving environment.  
32  
33  
34  
35  
36  
37  
38  
39  
40  
41  
42  
43  
44  
45  
46  
47  
48  
49  
50  
51  
52  
53  
54  
55  
56  
57  
58  
59  
60  
61  
62  
63  
64  
65

1 There are different automated analytical systems based on continuous flow methodologies and  
2 different detection techniques capable of determining orthophosphate in water, such as visible  
3 and fluorescence spectrophotometry, atomic spectrometry and electrochemistry, among others  
4 [2,11–15]. The spectrophotometric determination of phosphomolybdenum blue (PMB)  
5 complex, is one of the most commonly used standard methods for this purpose [2,16]. It  
6 consists in the reaction between orthophosphate and molybdate to produce 12-  
7 molybdophosphoric acid (12-MPA) in an acidic medium, which is then reduced to a PMB  
8 complex by means of ascorbic acid. PMB shows a broad absorption band ranging from 600 to  
9 900 nm [16–18]. Most of the automated systems based on the PMB reaction present some  
10 advantages regarding other methods, such as a relative short analysis time, low sample and  
11 reagent consumption and good reproducibility of the measurements. However, they are  
12 characterized by narrow working ranges, which limits their capacity to determine  
13 orthophosphate concentrations at the different stages of a WWTP, sometimes require skilled  
14 personnel for calibration purposes and, mostly all are high volume and weight equipment that  
15 cannot operate in field. [18–27]. In this sense, miniaturization of analytical systems to the so-  
16 called micro Total Analysis Systems ( $\mu$ TAS) can overcome these drawbacks [28,29]. In  
17 addition, the implementation of flow management systems based on multicommutation and  
18 multipumping techniques, using micropumps and microvalves, permits to fulfill the required  
19 miniaturization as well as the automation of the whole experimental setup thus, enabling  
20 autocalibration and autosampling [11,30].

21 The main component of a  $\mu$ TAS is a microfluidic platform which integrates all the different  
22 analytical operations in a single substrate. Polymer technology, and in particular Cyclic Olefin  
23 Copolymer (COC) technology, offers great advantages over other fabrication techniques and  
24 materials (glass, silicon or ceramics). Regarding material properties, COC shows good  
25 transparency in the UV-Vis range, good mechanical and chemical resistance and high  
26 biocompatibility. As for fabrication technology, it allows easy prototyping, low cost production,  
27  
28  
29  
30  
31  
32  
33  
34  
35  
36  
37  
38  
39  
40  
41  
42  
43  
44  
45  
46  
47  
48  
49  
50  
51  
52  
53  
54  
55  
56  
57  
58  
59  
60  
61  
62  
63  
64  
65

1 and the ability to easily obtain sealed multilayered devices without the need for adhesives [31–  
2 33].  
3

4 Detection systems must be also miniaturized to improve portability. The use of light-emitting  
5 diodes (LEDs) and small but sensitive detectors such as photodiodes, allow reducing the whole  
6 experimental setup dimensions compared to the conventional optical equipment. [34,35].  
7  
8

9  
10  
11 Herein, we propose a portable, automated, and compact experimental setup to determine SRP as  
12 orthophosphate in wastewater samples. This equipment consists of a COC-based microanalyzer,  
13 a miniaturized optical detection system and a flow management system, all computer controlled.  
14  
15 The microanalyzer integrates the required microfluidics to perform the PMB reaction and an  
16 optical detection cell. The detection system consists of a LED and a photodiode integrated in a  
17 PCB and the flow system is based on microvalves and micropumps programmed to allow  
18 autocalibration and autosampling. All this grants the required features to be implemented in  
19 municipal WWTP for SRP monitoring with a high potential for operation in unattended  
20 conditions. To verify its applicability, different real samples have been analyzed.  
21  
22

## 23 **2. Experimental**

### 24 *2.1. Reagents and materials*

25 All reagents employed in this work were of analytical grade. All solutions were prepared in  
26 double distilled water. Orthophosphate standard solutions were prepared by dilution using  
27 multicommutation sequences of a previously degassed 32 mg L<sup>-1</sup> P stock solution prepared from  
28 NaH<sub>2</sub>PO<sub>4</sub> (Fluka).  
29

30 As complexing and reducing solutions, 5 mM (NH<sub>4</sub>)<sub>6</sub>Mo<sub>7</sub>O<sub>24</sub>·4H<sub>2</sub>O (ammonium molybdate)  
31 (Fluka) with 0.1M H<sub>2</sub>SO<sub>4</sub> (Sigma-Aldrich) and 60 mM ascorbic acid (Sigma-Aldrich) were  
32 used, respectively.  
33

34 The microanalyzer was fabricated with plaques and foils of COC purchased from Topas  
35 Advanced Polymers (Florence, KY, USA) in different grades and thicknesses: Topas 5013  
36 plaques of 500 μm and 1 mm thick, and Topas 8007 foils of 25 μm thick.  
37  
38  
39  
40  
41  
42  
43  
44  
45  
46  
47  
48  
49  
50  
51  
52  
53  
54  
55  
56  
57  
58  
59  
60  
61  
62  
63  
64  
65

## 2.2. Fabrication of the microanalyzer

The fabrication of the microanalyzer is based on a multilayer approach, which is described in detail elsewhere [36–38]. It consists in the lamination of different COC machined layers with different glass transition temperatures ( $T_g$ ). Topas 5013 plaques with  $T_g=130\text{ }^\circ\text{C}$  were used as structural layers and machined with the designed patterns (microchannels and flow cell) and Topas 8007 foils with  $T_g=75\text{ }^\circ\text{C}$  were used as sealant layers between structural layers. The fabrication process in this case consists in four main steps: prototype design, pre-lamination step, pattern machining and final lamination. The design of the microanalyzer was carried out using CAD software. The microsystem was fabricated using 3 structural and two sealant layers so that, once overlapped in the correct order provided the three-dimensional structure required for the PMB reaction (Figure 1A). Microanalyzer dimensions were 30 x 50 x 2.5 mm, quite smaller than a credit card, and it weighted 3 g. Microfluidics inside the microanalyzer includes three inlets (Figure 2) and one outlet. First of all, complexing solution (ammonium molybdate in an acidic medium) and water (as carrier solution of samples or standard solutions), converge in a Y-shaped confluence point and get mixed along a small section of a serpentine micromixer, which generates 12-molybdophosphoric acid (12-MPA) if the carrier contains inorganic phosphate species ( $\text{H}_3\text{PO}_4$  to  $\text{PO}_4^{3-}$ ). Then, reducing solution (ascorbic acid) is introduced to the mixed stream to form the complex PMB, which develops a blue coloration along a larger serpentine section until reaching a flow-cell, where absorbance at 660 nm is measured. The stream is finally carried to the waste outlet.

All patterns (holes and microchannels) were machined onto the structural polymeric plaques (previously laminated with Topas 8007 foils) by means of a computer numerically controlled (CNC) micromilling machine (Protomat C100/HF, LPKF, Spain). The dimensions of the microchannels throughout the microsystem were 0.8 mm width and 1 mm height before the flow-cell and 0.4 mm width and 1 mm height after it. The diameter of the detection flow-cell was of 4.5 mm with an optical path-length of 1 mm. The total microsystem dead volume was of 326  $\mu\text{L}$ .

1 COC layers alignment and final lamination was performed in a thermo-compression press  
2 (Francisco Camps, Granollers, Spain) at 102 °C and 4 atm using an aluminum support with 4  
3 fiducial alignment pins. Thus, the whole microsystem became a monolithic substrate with the  
4 different layers perfectly sealed and without leakages. Finally, fluidic connectors were fixed  
5 onto the inlet/outlet ports of the microanalyzer with a holder and screws (Figure 1B).  
6  
7  
8  
9

### 10 *2.3. Experimental setup*

11  
12 The experimental setup consists of three main parts: the developed microanalyzer, the flow  
13 management system and the optical detection system. The flow management system setup is  
14 shown in the schematic diagram in Figure 2. It consists of two solenoid micro-pumps of 10 µL  
15 per pulse (P/N 120SP1210-5TP, BiochemValve Inc., Montluçon Cedex, France), one peristaltic  
16 micro-pump (Kamoer KP-S10DGC0, Shanghai, China) with a customized rpm controller (TMI,  
17 Barcelona, Spain) using Tygon® tubing (Ismatec, Wertheim, Germany) with 0.19 mm internal  
18 diameter, and three three-way solenoid valves (161T031, NResearch, Switzerland). Teflon  
19 tubing (Scharlab, S. L., Cambridge, England) of 0.8 mm internal diameter was used to connect  
20 the different flow elements to the microsystem. A controller for fluid elements (Flowtest™,  
21 Biotray, France) with its corresponding CosDesigner™ software was used in order to program  
22 microvalves and micropumps actuation for autocalibration by multicommutation and for  
23 automating the whole analytical procedure.  
24  
25  
26  
27  
28  
29  
30  
31  
32  
33  
34  
35  
36  
37  
38  
39  
40

41 As for the detection system (Figure 3), it consists of a compact and robust optical reader for  
42 microfluidic platforms, which was previously developed by our research group and described  
43 elsewhere [34,35]. It is composed by a structure that holds a Printed Circuit Board (PCB) with  
44 the optical detection electronics and an insertion port, designed with a lock and key concept.  
45  
46  
47  
48  
49

50 This insertion port has the complementary shape of the microanalyzer in order to allow a perfect  
51 alignment between the light source, the measurement flow-cell and the detector (Figure 3B).  
52  
53

54 The PCB structure integrates as a light source a Light Emitting Diode (LED) with an emission  
55 peak centered at 660 nm (Kingbright, Taipei, Taiwan) and as a detector, a PIN Hamamatsu  
56 S1337-66BR large active area photodiode. By means of a Data Acquisition Card (DAQ) NI  
57  
58  
59  
60  
61  
62  
63  
64  
65

1 USB-6211 from National Instruments (Austin, Texas, US), the signal generated was acquired  
2 and transferred via USB interface, to a personal computer, where it was processed using a  
3 digital lock-in amplifier, which increased the signal-to noise ratio and allowed working in  
4 ambient light conditions with no alterations on the measurements.  
5  
6

### 7 **3. Results and discussion**

#### 8 *3.1. Design and optimization of the analytical microsystem*

9  
10  
11 The main goal of this work is the development of a portable, automatic, compact and computer  
12 controlled full experimental setup; composed by a microanalyzer, a flow management system  
13 and a detection system; for the determination of SRP at different stages of the water purification  
14 process in municipal WWTP. Other key features to fulfill are low cost, simplicity, robustness  
15 and low reagents consumption, whereas analytical features such as selectivity and a large  
16 working range in short analysis time must be also attained.  
17  
18

19 Microfluidics was designed considering previous experience to procure maximum sensitivity  
20 and selectivity with low reagents consumption and avoiding the formation of PMB precipitate.  
21

22 Flow-cell configuration was designed and optimized, following our previous works [38], by  
23 introducing smooth-contour geometries to prevent the formation and retention of bubbles, thus  
24 increasing the overall robustness of the microsystem avoiding distortions in the measurements.  
25

26 The first section of the micromixer, where 12-MPA is formed, had a short length in order to  
27 avoid the potential interfering effect of the silicate (the largest interfering compound of this  
28 analytical method present in wastewater) [2]. As kinetics favors the formation of  
29 phosphomolybdate instead of silicomolybdate [2,39], the shorter the reaction time prior the  
30 reduction, the less interference of silicate. On the other hand, since the reduction of 12-MPA to  
31 PMB has slower kinetics than the previous reaction (no catalyzer is employed to reduce costs,  
32 enlarge the working range, avoid the precipitation of PMB and solve other reagents stability  
33 problems), the length of the second section of the micromixer was larger. At a given chemical  
34 and hydrodynamics parameters values, longer micromixers would lead to higher concentrations  
35 of PMB and enhance the signal, but, in turn the possibility of PMB to precipitate increased,  
36  
37  
38  
39  
40  
41  
42  
43  
44  
45  
46  
47  
48  
49  
50  
51  
52  
53  
54  
55  
56  
57  
58  
59  
60  
61  
62  
63  
64  
65

1 which could deposit on the microchannel walls or in the detection cell, causing a continuous  
2 drift of the baseline and possible clogging. Likewise, turbidity would increase so as the optical  
3 noise. The designed length of the micromixers assured a wide linear range and an adequate  
4 sensitivity and robustness for the application studied although the reduction time is far from the  
5 values necessary to obtain the maximum absorbance. Taking into account the micromixers  
6 dimensions and the optimization of the chemical and hydrodynamic variables (explained  
7 below), the reaction times for the complexation and reduction reactions were 3s and 12s,  
8 respectively.  
9

10 The microfluidic platform shape was designed to be inserted into the detection system based on  
11 a lock and key concept (Figure 3), allowing a perfect alignment between the LED, the flow-cell  
12 and the photodiode.  
13

14 Different LEDs emitting at different wavelengths (between 660 and 700 nm) were tested to  
15 follow the production of PMB, which has a broad absorption band ranging from 500 to 1100 nm  
16 [17,18]. The best option in terms of sensitivity, working range, cost and baseline stability was  
17 the LED with the emission peak centered at 660 nm, as it was previously reported [22].  
18

19 The influence of chemical variables (complexing solution, reducing solution and interfering  
20 compounds) and hydrodynamic parameters (flow rate and sample injection volume) on the  
21 analytical features were evaluated using an optimization procedure for each variable  
22 individually as a compromise between selectivity, sensitivity, baseline signal stability, linear  
23 working range, reagent consumption, reagents stability and analysis time. For the complexing  
24 solution, ammonium molybdate in sulfuric acid was selected according to published features  
25 regarding sensitivity and working range [2]. Ammonium molybdate was tested at concentrations  
26 ranging from 2.5 to 15 mM and sulfuric acid was evaluated from 0 to 0.5 M. The optimal results  
27 were obtained using 5mM ammonium molybdate with 0.1M sulfuric acid. As reducing agent,  
28 ascorbic acid was selected as it may allow a wider working range and its cost and stability are  
29 better than other reagents such as  $\text{SnCl}_2$  [40]. The concentration of ascorbic acid was evaluated  
30 from 5 to 120 mM. It was observed that above 30 mM, the absorbance caused by a determined  
31  
32  
33  
34  
35  
36  
37  
38  
39  
40  
41  
42  
43  
44  
45  
46  
47  
48  
49  
50  
51  
52  
53  
54  
55  
56  
57  
58  
59  
60  
61  
62  
63  
64  
65

1 concentration of phosphate was practically the same, however at concentrations below 30mM  
2 the absorbance decreased dramatically. Since the reducing agent breaks down relatively easily,  
3 it was used in great excess (60 mM) in order to prevent the decrease of the measured absorbance  
4 in case of reagent degradation. In addition, ascorbic acid decomposes faster in acidic medium  
5 [41] so, it was always prepared and stored at neutral pH. Thus, the stability of the reducing  
6 solution over time was increased.

7  
8  
9  
10  
11  
12  
13 Regarding the potential interfering compounds of the PMB method, silicate, arsenate and  
14 germanate are compounds that can produce molybdenum complexes with similar absorption  
15 wavelength as PMB complex [2]. However, only silicate can be found in significant  
16 concentration in wastewater. As it has been stated previously, taking profit from the favorable  
17 kinetics of PMB complex formation in an acidic medium versus the silicomolybdate complex  
18 and the presented microfluidic design and hydrodynamic parameters selected, this interfering  
19 effect was minimized to an 11 % of overestimation in a 1:10 (P:Si) ratio at 3.2 mg L<sup>-1</sup> P.

20  
21  
22  
23  
24  
25  
26  
27  
28  
29  
30  
31  
32  
33  
34  
35  
36  
37  
38  
39  
40  
41  
42  
43  
44  
45  
46  
47  
48  
49  
50  
51  
52  
53  
54  
55  
56  
57  
58  
59  
60  
61  
62  
63  
64  
65  
According to the literature [42], around 70% of the analyzed water samples have less than 10  
mg L<sup>-1</sup> Si, so the possible interfering effect would be less than 6 % of overestimation. Whether  
samples contained higher silicate concentration or a significant interfering effect, masking  
agents such as oxalic or tartaric acid could be previously added to eliminate completely the  
interfering effects as it has been confirmed in numerous works [2,11,16,17,43], however, this  
would increase reagent costs.

Hydrodynamics optimization was performed with different flow rates and sample injection  
volumes. Flow rates between 100-500  $\mu\text{L min}^{-1}$  (for each channel) and sample injection  
volumes from 50-1000  $\mu\text{L}$  were tested. The optimal results were obtained using a flow rate of  
400  $\mu\text{l min}^{-1}$  for each channel and a sample injection volume of 133  $\mu\text{L}$ .

### 3.2. *Flow System*

The automation and miniaturization of the whole analytical system provides with great  
autonomy and versatility. Monitoring SRP at different stages of a WWTP or even in threatened

1 water bodies can be done under unattended conditions. In this way, it is possible to drastically  
2 reduce costs in terms of consumption of reagents, equipment and specialized personnel.

3  
4 Therefore, a computer-controlled flow management system was implemented. It is a hybrid  
5  
6 proposal based on multicommutation and multipumping systems, which combines solenoid  
7  
8 micropumps and microvalves and a peristaltic micropump, all managed with a controller  
9  
10 (Flowtest™), as was stated previously [44,45]. This flow management system also allowed a  
11  
12 programmable modulation/modification of the hydrodynamic parameters to customize the  
13  
14 analytical characteristics (linear working range, detection limit, sensitivity, etc.) to special or  
15  
16 exceptional conditions not initially foreseen, such as great variations in the expected  
17  
18 orthophosphate concentration.  
19  
20

21  
22  
23 Using a solenoid microvalve and a peristaltic micropump, an automated calibration process was  
24  
25 performed, preparing the different standard solutions by multicommutation dilution from a  
26  
27 single concentrated stock solution. Technical parameters such as the injection time (related to  
28  
29 the volume of injection in this type of systems), the minimum operation time of the microvalve  
30  
31 and the pumping system used, determine the accuracy of the dilution process. Thus, the highest  
32  
33 commutation speed (on/off) of the solenoid microvalve was set at 100 ms [44,46]. With this  
34  
35 configuration, dilution factors of 200 times the concentration of the original stock solution could  
36  
37 be achieved.  
38  
39

40  
41  
42 Table 1 shows the different standard solutions generated and how they were made from a 32 mg  
43  
44 L<sup>-1</sup> P stock solution. With an optimized flow rate of 400 μL min<sup>-1</sup>, the optimized injection time  
45  
46 to get the 133 μL of sample injection volume was 20 s. As an example, when a 32 mg L<sup>-1</sup> P  
47  
48 standard solution is to be injected to the microsystem, the stock solution is introduced without  
49  
50 dilution during the 20 s of the injection time. On the other hand, when the 0.32 mg L<sup>-1</sup> P  
51  
52 standard solution is injected, during the 20 s of the injection time, 2 cycles are carried out in  
53  
54 which the stock solution is introduced for 0.1 s (“on” position of the microvalve ) and water is  
55  
56 introduced for the remaining 9.9 s (“off” position of the microvalve). Valve 3 (V<sub>3</sub>, Figure 2) is  
57  
58  
59  
60  
61  
62  
63  
64  
65

1 only used when solutions should not reach the flow-cell, during the initial system filling or for  
2 sample changing.  
3

4 In order to verify the correct operation of the automated standard solutions preparation by  
5 multicommutation sequences of dilution from a stock solution, the prepared solutions were  
6 compared with hand-made standard solutions. Results showed no significant differences  
7 between both types of standard solutions with RSD values lower than 3%.  
8  
9  
10  
11  
12

### 13 *3.3. Analytical performance*

14 Analytical microsystem characterization was carried out by different calibrations obtained using  
15 the automated dilution program from the stock solution of 32 mg L<sup>-1</sup> P. Figure 4 shows the  
16 obtained recorded signal for one of these performed calibrations. The obtained response  
17 function ( $n = 9$  and 95% confidence) was  $A = 0.4 (\pm 0.2) + 3.18 (\pm 0.02) [P]$  with  $r^2=0.9996$ .  
18 Detection limit, calculated as three times the standard deviation of the blank, was 0.03 mg L<sup>-1</sup> P,  
19 while linear working range ( limit of quantification calculated as 10 times the standard deviation  
20 of the blank) was 0.09 to 32 mg L<sup>-1</sup> P. Repeatability studies were performed by successive  
21 injections of a 3.2 mg L<sup>-1</sup> P standard solution. Relative standard deviation ( $n = 6$ , 95%  
22 confidence) of the signal was lower than 1%.  
23  
24  
25  
26  
27  
28  
29  
30  
31  
32  
33  
34  
35  
36  
37

38 Reproducibility between different days along 3 months using the same reagent solutions was  
39 also determined. A mean slope of the response function of 2.99 mAU · L · mg<sup>-1</sup> ( $n=5$ ) with a RSD  
40 value lower than 6% was achieved, thus demonstrating the reproducible inter-day validation of  
41 the microsystem and the good stability of the selected reagents. A sampling rate of 24 samples  
42 h<sup>-1</sup> was obtained with the optimized experimental conditions. These results also showed the  
43 robustness and the reliability of the whole experimental setup and its potential to be used in the  
44 analysis of SRP in both wastewater samples in WWTPs and natural water samples from rivers  
45 or lakes.  
46  
47  
48  
49  
50  
51  
52  
53  
54  
55  
56

### 57 *3.4. Real samples analysis*

1 Real samples collected from different sampling points of the treatment stages of a municipal  
2 wastewater treatment plant (Guardamar del Segura, Alicante, Spain) were analyzed using the  
3 developed microsystem in order to determine the SRP content. This phosphorus fraction is an  
4 indicator to manage and optimize the quantity of necessary reagents for the phosphorus removal  
5 in the different stages in WWTPs. Moreover, at the final stage it is a clear indicator of the  
6 possible eutrophication in the receiving water bodies. There are different phosphorus fractions  
7 that can be analyzed with the proposed microanalyzer, depending on the pretreatment that is  
8 performed on the sample [2]. The soluble reactive phosphorus fraction (SRP) comprises all  
9 species of inorganic phosphorus in solution after subjecting the sample to a filtration process  
10 with a 0.45  $\mu\text{m}$  pore size filter. Thus, the particulate reactive phosphorus (PRP) is removed.  
11 SRP and PRP are the total reactive phosphorous (TRP) [2,47]. It is important to assure that the  
12 sample to be analyzed does not contain PRP, in order to avoid alterations in the obtained results.  
13 In this work, with the objective of simplifying the analytical process, the filtration stage was  
14 suppressed, assuming that decantation of the PRP for 5 minutes allowed a reliable measurement  
15 of the SRP, free of other phosphorus fractions. Since all potential sampling points in a WWTP  
16 are located or related to deposits, pools or areas where a decantation process can be carried out,  
17 this should not be a problem to implement the microanalyzer in routine analysis in WWTPs.  
18 However, if other types of phosphorus fractions were required to be analyzed, different stages of  
19 hydrolysis or digestion should be performed, which could be easily introduced into the analysis  
20 process [2,11]. In order to verify that the decantation process was efficient to separate PRP from  
21 SRP, the analysis of the same sample obtained by decantation and filtration was performed.  
22 Similar results were obtained;  $5.7 \pm 0.6 \text{ mg L}^{-1} \text{ P}$  (n=3, 95% confidence) in filtered samples and  
23  $5.9 \pm 0.3 \text{ mg L}^{-1} \text{ P}$  (n=3, 95% confidence) in decanted samples. This confirmed that the  
24 decantation process was sufficient to determine only the fraction of SRP in that type of water.  
25 However, further analysis with a larger set of samples should be conducted to feasibly  
26 demonstrate this statement.

1 Results obtained from the analysis of different samples with the proposed miniaturized analyzer  
2 were validated by comparison with the ones obtained with inductively coupled plasma optical  
3 emission spectrometry (ICP-OES). The obtained results are shown in Table 2.  
4  
5

6  
7 As it can be seen, results obtained with the developed microanalyzer are not significantly  
8 different from the ones obtained with the reference method using the paired t-test ( $t_{\text{calc}} = 0.382$ ;  
9  $t_{\text{tab}} = 1.833$ ;  $t_{\text{calc}} < t_{\text{tab}}$ ). This fact confirmed that the proposed system is useful for the  
10 determination of SRP in a wide range of concentrations, allowing its monitoring throughout the  
11 different stages of the WWTP (phosphorous can vary considerably from one stage to another).  
12  
13  
14  
15  
16  
17

#### 18 **4. Conclusions**

19  
20 A low cost and compact microanalyzer for the automated spectrophotometric determination of  
21 SRP was designed, developed, characterized and applied to the analysis of real samples of a  
22 WWTP. The microsystem was optimized in order to maximize operational autonomy and  
23 lifetime and to achieve a good analytical performance, with no need for pretreatment sample  
24 stages such as filtration, and including an autocalibration process based on the in-situ  
25 preparation of the standard calibration solutions by a multicommutation strategy based on the  
26 dilution of a stock standard solution. The presented set up is robust and miniaturized and  
27 provides a fast response with low sample and reagents consumption. It allows measuring SRP  
28 with a wider working range than other analytical systems published to date for orthophosphate  
29 analysis in wastewater. The integration of an automatic fluid management system, based on  
30 microvalves and micropumps, improves the automation and the miniaturization of the whole  
31 experimental setup, making it more suitable for an unattended analysis of SRP in WWTP.  
32  
33 Likewise, the use of an optical reader consisting of a LED and a PIN-photodiode as an optical  
34 detection system, where the microanalyzer can be inserted based on a lock and key concept, also  
35 contributed to achieve these characteristics.  
36  
37  
38  
39  
40  
41  
42  
43  
44  
45  
46  
47  
48  
49  
50  
51  
52  
53  
54

55  
56  
57 The analytical features of the microanalyzer meet the established requirements, being suitable as  
58 well for remote autonomous stations to follow eutrophication processes of sensitive water  
59  
60  
61  
62  
63  
64  
65

1 bodies as for the online monitoring of phosphate ion in WWTPs to efficiently determine  
2 chemical or biological reagent dosages necessary to remove phosphorus from treated water [48].  
3  
4 In this sense, a smart valve could be implemented so that at high SRP levels in the effluent of a  
5  
6 WWTP, the effluent were recirculated and not discharged to the water bodies, thus avoiding the  
7  
8 ecosystem hypernutrition that could trigger specific episodes of eutrophication.  
9

### 10 11 **CRedit author statement**

12  
13  
14 Antonio Calvo-Lopez: Conceptualization, Microsystem design and fabrication,  
15  
16  
17 Methodology, Investigation, Formal analysis, Validation and Writing - Original Draft.  
18

19  
20 Oriol Ymbern: Microsystem design and Detection system design and fabrication.  
21

22  
23 Mar Puyol: Conceptualization, Funding acquisition and administration and Writing -  
24  
25 Review & Editing.  
26

27  
28 Julian Alonso-Chamarro: Conceptualization, Resources, Writing - Review & Editing,  
29  
30 Supervision, Project administration and Funding acquisition.  
31

### 32 33 **Conflicts of interest**

34  
35  
36  
37 The authors declare that they have no known competing financial interests or personal  
38  
39 relationships that could have appeared to influence the work reported in this paper.  
40  
41

### 42 43 **Funding**

44  
45  
46 This work was supported by Spain's Ministry of Economy and Competitiveness through the  
47  
48 project MINECO-FEDER CTQ2017-85011-R and to Catalan government through the project  
49  
50 2017SGR 220.  
51

### 52 53 **Acknowledgments**

54  
55  
56  
57 The authors would like to thank A. Blasco from the Guardamar del Segura wastewater treatment  
58  
59 plant for providing the municipal wastewater samples.  
60  
61

## References

- 1  
2  
3 [1] American Public Health Association, American Water Works Association, Water  
4 Environment Federation, Standard Methods for the examination of water and  
5 wastewater, 22nd ed., American Public Health Association, Washington, DC., 2017.  
6  
7  
8  
9  
10 [2] L.M.L. Nollet, Handbook of Water Analysis, 2nd ed., Taylor & Francis Group, Boca  
11 Raton, Florida, 2007. doi:10.1038/006104a0.  
12  
13  
14  
15 [3] S.R. Carpenter, N.F. Caraco, D.L. Correll, R.W. Howarth, A.N. Sharpley, V.H. Smith,  
16 Nonpoint Pollution of Surface Waters with Phosphorus and Nitrogen, *Ecol. Appl.* 820  
17 (1998) 559–568.  
18  
19  
20  
21  
22 [4] A.A. Ansari, S.S. Gill, G.R. Lanza, W. Rast, *Eutrophication: causes, consequences and*  
23 *control*, Springer, New York, 2011.  
24  
25  
26  
27 [5] L.G. Huffman, *Evaluating Eutrophication Control Alternatives for the Lower Neuse*  
28 *River, North Carolina*, University of Virginia, 1988.  
29  
30  
31  
32 [6] A. Tekile, I. Kim, J. Kim, Mini-review on river eutrophication and bottom improvement  
33 techniques, with special emphasis on the Nakdong River, *J. Environ. Sci. (China)*. 30  
34 (2015) 113–121. doi:10.1016/j.jes.2014.10.014.  
35  
36  
37  
38  
39 [7] M. Von Sperling, *Wastewater characteristics, treatment and disposal*, 1st editio, IWA  
40 Publishing, London, UK, 2007. doi:10.5860/CHOICE.45-2633.  
41  
42  
43  
44 [8] M. Henze, Y. Comeau, *Wastewater Characterization*, in: *Biol. Wastewater Treat. Princ.*  
45 *Model. Des.*, IWA Publishing, London, UK, 2008: pp. 33–52.  
46  
47  
48  
49 [9] W. García, Basic wastewater characteristics, *Pipeline*. 8 (1997) 1–8.  
50  
51  
52 [10] W. Xiaolian, P. Yongzhen, W. Shuying, F. Jie, C. Xuemei, Influence of wastewater  
53 composition on nitrogen and phosphorus removal and process control in A2O process,  
54 *Bioprocess Biosyst. Eng.* 28 (2006) 397–404. doi:10.1007/s00449-006-0044-5.  
55  
56  
57  
58  
59 [11] J.M. Estela, V. Cerdà, Flow analysis techniques for phosphorus: An overview, *Talanta*.  
60  
61  
62  
63  
64  
65

66 (2005) 307–331. doi:10.1016/j.talanta.2004.12.029.

- 1  
2  
3 [12] M. Bowden, D. Diamond, The determination of phosphorus in a microfluidic manifold  
4 demonstrating long-term reagent lifetime and chemical stability utilising a colorimetric  
5 method, *Sensors Actuators, B Chem.* 90 (2003) 170–174. doi:10.1016/S0925-  
6 4005(03)00024-8.  
7  
8  
9  
10  
11 [13] M.M. Villalba, K.J. McKeegan, D.H. Vaughan, M.F. Cardosi, J. Davis,  
12 Bioelectroanalytical determination of phosphate: A review, *J. Mol. Catal. B Enzym.* 59  
13 (2009) 1–8. doi:10.1016/j.molcatb.2008.12.011.  
14  
15  
16  
17 [14] F.E. Legiret, V.J. Sieben, E.M.S. Woodward, S.K. Abi Kaed Bey, M.C. Mowlem, D.P.  
18 Connelly, E.P. Achterberg, A high performance microfluidic analyser for phosphate  
19 measurements in marine waters using the vanadomolybdate method, *Talanta.* 116 (2013)  
20 382–387. doi:10.1016/j.talanta.2013.05.004.  
21  
22  
23  
24 [15] S. Motomizu, Z.H. Li, Trace and ultratrace analysis methods for the determination of  
25 phosphorus by flow-injection techniques, *Talanta.* 66 (2005) 332–340.  
26 doi:10.1016/j.talanta.2004.12.056.  
27  
28  
29  
30 [16] E.A. Nagul, I.D. McKelvie, P. Worsfold, S.D. Kolev, The molybdenum blue reaction for  
31 the determination of orthophosphate revisited: Opening the black box, *Anal. Chim. Acta.*  
32 890 (2015) 60–82. doi:10.1016/j.aca.2015.07.030.  
33  
34  
35  
36 [17] J. Murphy, J.P. Riley, A modified single solution method for the determination of  
37 phosphate in natural waters, *Anal. Chim. Acta.* 27 (1962) 31–36. doi:10.1016/S0003-  
38 2670(00)88444-5.  
39  
40  
41  
42 [18] M. Fiedoruk, E. Mieczkowska, R. Koncki, Ł. Tymecki, A bimodal optoelectronic flow-  
43 through detector for phosphate determination, *Talanta.* 128 (2014) 211–214.  
44 doi:10.1016/j.talanta.2014.04.086.  
45  
46  
47  
48 [19] R.N.C. Daykin, S.J. Haswell, Development of a micro flow injection manifold for the  
49 determination of orthophosphate, *Anal. Chim. Acta.* 313 (1995) 155–159.  
50  
51  
52  
53  
54  
55  
56  
57  
58  
59  
60  
61  
62  
63  
64  
65

doi:10.1016/0003-2670(95)00393-E.

- 1  
2  
3 [20] E.A.M. Kronka, B.F. Reis, M. Korn, F.H. Bergamin, Multicommutation in flow analysis.  
4 Part 5: Binary sampling for sequential spectrophotometric determination of ammonium  
5 and phosphate in plant digests, *Anal. Chim. Acta.* 334 (1996) 287–293.  
6  
7 doi:10.1016/S0003-2670(96)00267-X.  
8  
9  
10  
11 [21] G.N. Doku, S.J. Haswell, Further studies into the development of a micro-FIA system  
12 based on electroosmotic flow for the determination of phosphate as orthophosphate,  
13 *Anal. Chim. Acta.* 382 (1999) 1–13. doi:10.1016/S0003-2670(98)00830-7.  
14  
15  
16  
17 [22] R.N. Fernandes, B.F. Reis, Flow system exploiting multicommutation to increase sample  
18 residence time for improved sensitivity. Simultaneous determination of ammonium and  
19 ortho-phosphate in natural water, *Talanta.* 58 (2002) 729–737. doi:10.1016/S0039-  
20 9140(02)00369-7.  
21  
22  
23  
24 [23] M. Hatta, C.I. Measures, J. (Jarda) Ruzicka, Determination of traces of phosphate in sea  
25 water automated by programmable flow injection: Surfactant enhancement of the  
26 phosphomolybdenum blue response, *Talanta.* 191 (2019) 333–341.  
27  
28 doi:10.1016/j.talanta.2018.08.045.  
29  
30  
31 [24] J.C. Yan, J. Ren, L.L. Ren, J.M. Jian, Y. Yang, S.F. Yang, T.L. Ren, Development of a  
32 portable setup using a miniaturized and high precision colorimeter for the estimation of  
33 phosphate in natural water, *Anal. Chim. Acta.* 1058 (2019) 70–79.  
34  
35  
36 doi:10.1016/j.aca.2019.01.030.  
37  
38  
39 [25] W. Khongpet, S. Pencharee, C. Puangpila, S. Kradtap Hartwell, S. Lapanantnoppakhun,  
40 J. Jakmune, Exploiting an automated microfluidic hydrodynamic sequential injection  
41 system for determination of phosphate, *Talanta.* 177 (2018) 77–85.  
42  
43  
44  
45 doi:10.1016/j.talanta.2017.09.018.  
46  
47  
48  
49 [26] S. Koronkiewicz, M. Trifescu, L. Smoczynski, H. Ratnaweera, S. Kalinowski, A novel  
50 automatic flow method with direct-injection photometric detector for determination of  
51  
52  
53  
54  
55  
56  
57  
58  
59  
60  
61  
62  
63  
64  
65

- dissolved reactive phosphorus in wastewater and freshwater samples, *Environ. Monit. Assess.* 190 (2018). doi:10.1007/s10661-018-6511-z.
- [27] S. Karadağ, E.M. Görüşük, E. Çetinkaya, S. Deveci, K.B. Dönmez, E. Uncuoğlu, M. Doğu, Development of an automated flow injection analysis system for determination of phosphate in nutrient solutions, *J. Sci. Food Agric.* 98 (2018) 3926–3934. doi:10.1002/jsfa.8911.
- [28] A. Rios, A. Escarpa, B. Simonet, *Miniaturization in Analytical Chemistry*, JohnWiley & Sons, United Kingdom, 2009.
- [29] D.R. Reyes, D. Iossifidis, P.A. Auroux, A. Manz, *Micro total analysis systems. 1. Introduction, theory, and technology.*, *Anal. Chem.* 74 (2002) 2623–2636. <http://www.ncbi.nlm.nih.gov/pubmed/12090653>.
- [30] M. Trojanowicz, K. Kolacinska, *Recent Advances in Flow Injection Analysis*, *Analyst.* 141 (2016) 2085–2139.
- [31] J. Steigert, S. Haeberle, T. Brenner, C. Müller, C.P. Steinert, P. Koltay, N. Gottschlich, H. Reinecke, J. Rühle, R. Zengerle, J. Ducrée, *Rapid prototyping of microfluidic chips in COC*, *J. Micromechanics Microengineering.* 17 (2007) 333–341. doi:10.1088/0960-1317/17/2/020.
- [32] H. Becker, C. Gärtner, *Polymer microfabrication technologies for microfluidic systems.*, *Anal. Bioanal. Chem.* 390 (2008) 89–111. doi:10.1007/s00216-007-1692-2.
- [33] P.S. Nunes, P.D. Ohlsson, O. Ordeig, J.P. Kutter, *Cyclic olefin polymers: Emerging materials for lab-on-a-chip applications*, *Microfluid. Nanofluidics.* 9 (2010) 145–161. doi:10.1007/s10404-010-0605-4.
- [34] S.G. Pedro, M. Puyol, D. Izquierdo, I. Salinas, J.M. de la Fuente, J. Alonso-Chamarro, *A ceramic microreactor for the synthesis of water soluble CdS and CdS/ZnS nanocrystals with on-line optical characterization*, *Nanoscale.* 4 (2012) 1328. doi:10.1039/c2nr11525e.

- 1  
2  
3  
4  
5  
6  
7  
8  
9  
10  
11  
12  
13  
14  
15  
16  
17  
18  
19  
20  
21  
22  
23  
24  
25  
26  
27  
28  
29  
30  
31  
32  
33  
34  
35  
36  
37  
38  
39  
40  
41  
42  
43  
44  
45  
46  
47  
48  
49  
50  
51  
52  
53  
54  
55  
56  
57  
58  
59  
60  
61  
62  
63  
64  
65
- [35] O. Ymbern, M. Berenguel-Alonso, A. Calvo-López, S. Gómez-De Pedro, D. Izquierdo, J. Alonso-Chamarro, Versatile lock and key assembly for optical measurements with microfluidic platforms and cartridges, *Anal. Chem.* 87 (2015) 1503–1508. doi:10.1021/ac504255t.
- [36] O. Ymbern, N. Sáñez, A. Calvo-López, M. Puyol, J. Alonso-Chamarro, Gas diffusion as a new fluidic unit operation for centrifugal microfluidic platforms., *Lab Chip.* 14 (2014) 1014–22. doi:10.1039/c3lc51114f.
- [37] A. Calvo-López, O. Ymbern, M. Puyol, J.M. Casalta, J. Alonso-Chamarro, Potentiometric analytical microsystem based on the integration of a gas-diffusion step for on-line ammonium determination in water recycling processes in manned space missions, *Anal. Chim. Acta.* 874 (2015) 26–32. doi:10.1016/j.aca.2014.12.038.
- [38] A. Calvo-López, O. Ymbern, D. Izquierdo, J. Alonso-Chamarro, Low cost and compact analytical microsystem for carbon dioxide determination in production processes of wine and beer, *Anal. Chim. Acta.* 931 (2016) 64–69. doi:10.1016/j.aca.2016.05.010.
- [39] K. Grudpan, P. Ampan, Y. Udnan, S. Jayasvati, S. Lapanantnoppakhun, J. Jakmune, G.D. Christian, J. Ruzicka, Stopped-flow injection simultaneous determination of phosphate and silicate using molybdenum blue, *Talanta.* 58 (2002) 1319–1326. doi:10.1016/S0039-9140(02)00441-1.
- [40] J. Van der Merwe, J. van Staden, Evaluation of a number of methods for the determination of trace amounts of phosphates with flow injection analysis (FIA), *Water SA.* 23 (1997) 169–174.
- [41] J.-P. Yuan, F. Chen, Degradation of Ascorbic Acid in Aqueous Solution, *J. Agric. Food Chem.* 46 (1998) 5078–5082. doi:10.1021/jf9805404.
- [42] F. Armijo Castro, J. San Martín, M. Armijo Valenzuela, Contenido en sílice en algunas aguas minerales, *An. Bromatol.* (1979) 365–373.
- [43] R.A. Chalmers, A.G. Sinclair, Analytical applications of B-heteropoly acids: Part II,

Anal Chim Acta. 34 (1966) 412–418.

- 1  
2  
3 [44] A. Calvo-López, M. Puyol, J.M. Casalta, J. Alonso-Chamarro, Multi-parametric  
4 polymer-based potentiometric analytical microsystem for future manned space missions,  
5 Anal. Chim. Acta. (2017). doi:10.1016/j.aca.2017.08.043.  
6  
7  
8  
9  
10 [45] A. Calvo-López, Diseño, construcción y evaluación de analizadores miniaturizados para  
11 su aplicación aeroespacial, medioambiental, alimentaria, biomédica e industrial,  
12 Universitat Autònoma de Barcelona, 2017.  
13  
14  
15  
16 [46] Z.M. da Rocha, C.S. Martinez-Cisneros, A.C. Seabra, F. Valdés, M.R. Gongora-Rubio,  
17 J. Alonso-Chamarro, Compact and autonomous multiwavelength microanalyzer for in-  
18 line and in situ colorimetric determinations, Lab Chip. 12 (2012) 109.  
19  
20  
21  
22  
23  
24  
25  
26  
27 [47] S.M. Scherrenberg, Reaching ultra low phosphorus concentrations by filtration  
28 techniques (tesis doctoral), Technische Universiteit Delft, 2011.  
29  
30  
31 [48] G. Carty, G. O’Leary, B. Meaney, Wastewater Treatment Manuals. Primary, secondary  
32 and tertiary treatment., Environmental Protection Agency, Ireland, 1997.  
33  
34  
35  
36  
37  
38  
39  
40  
41  
42  
43  
44  
45  
46  
47  
48  
49  
50  
51  
52  
53  
54  
55  
56  
57  
58  
59  
60  
61  
62  
63  
64  
65

**Table 1:** Multicommutation dilution sequences to generate the different standard solutions from a 32 mg L<sup>-1</sup> stock solution.

Standard solution (mg L <sup>-1</sup> )	Total injection time (s)	Time on (stock solution) (s)	Time off (water) (s)	Cycles	Times diluted
32.00	20.0	20.0	0.0	0	0
16.00	20.0	0.1	0.1	200	2
8.00	20.0	0.1	0.3	40	4
3.20	20.0	0.1	0.9	20	10
1.60	20.0	0.1	1.9	10	20
0.80	20.0	0.1	3.9	5	40
0.32	20.0	0.1	9.9	2	100
0.16	20.0	0.1	19.9	1	200

**Table 2:** Mean concentration values in mg L<sup>-1</sup> (n=3, 95%) from the analysis of orthophosphate ion in wastewater samples using the proposed microsystem and the reference method.

Sample	Microsystem	ICP-OES	% difference
1	0.6 ± 0.2	0.5	20
2	23 ± 2	25.4	-9
3	3.8 ± 0.3	4.04	-6
4	19 ± 1	19.3	-2
5	5.1 ± 0.5	4.95	3
6	32 ± 2	31.1	3
7	5.7 ± 0.6	5.9	-3
8	3.2 ± 0.4	3.22	-1
9	31 ± 2	30.1	3

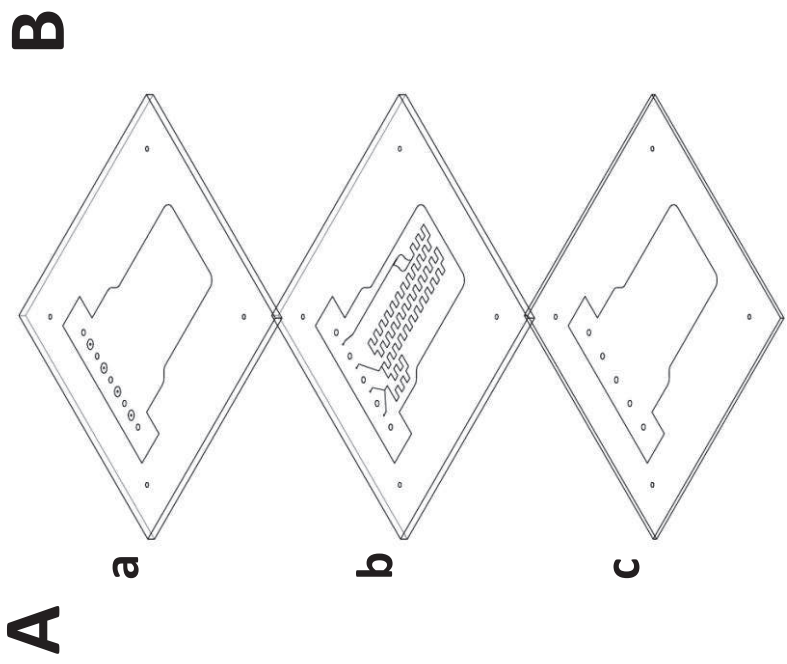
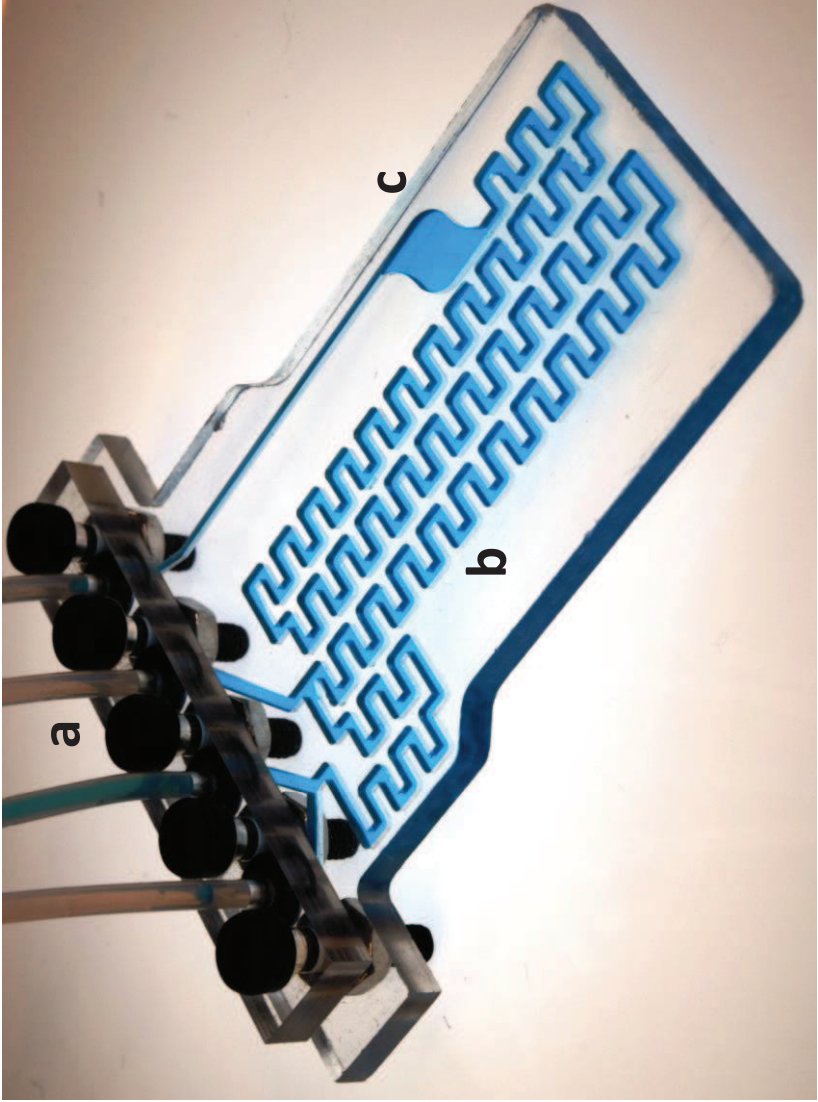
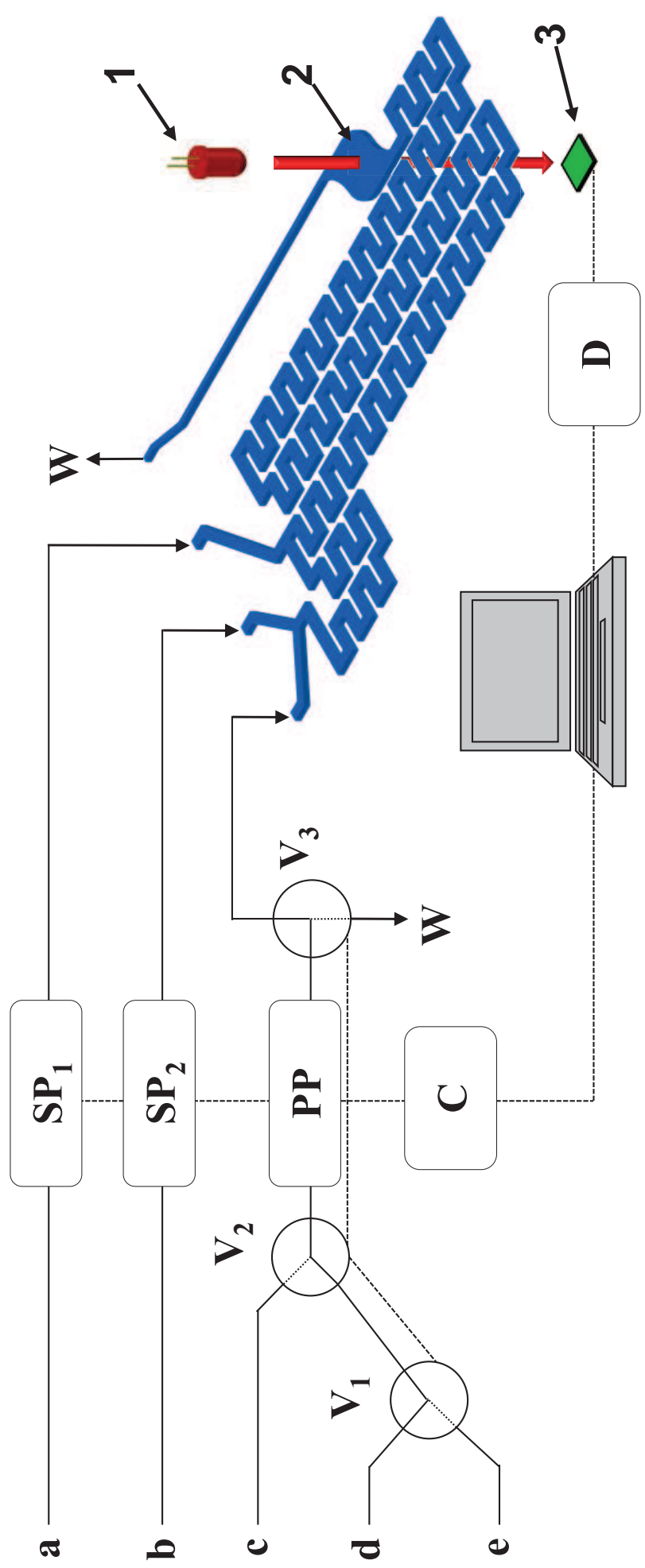


Figure 1

Figure 2



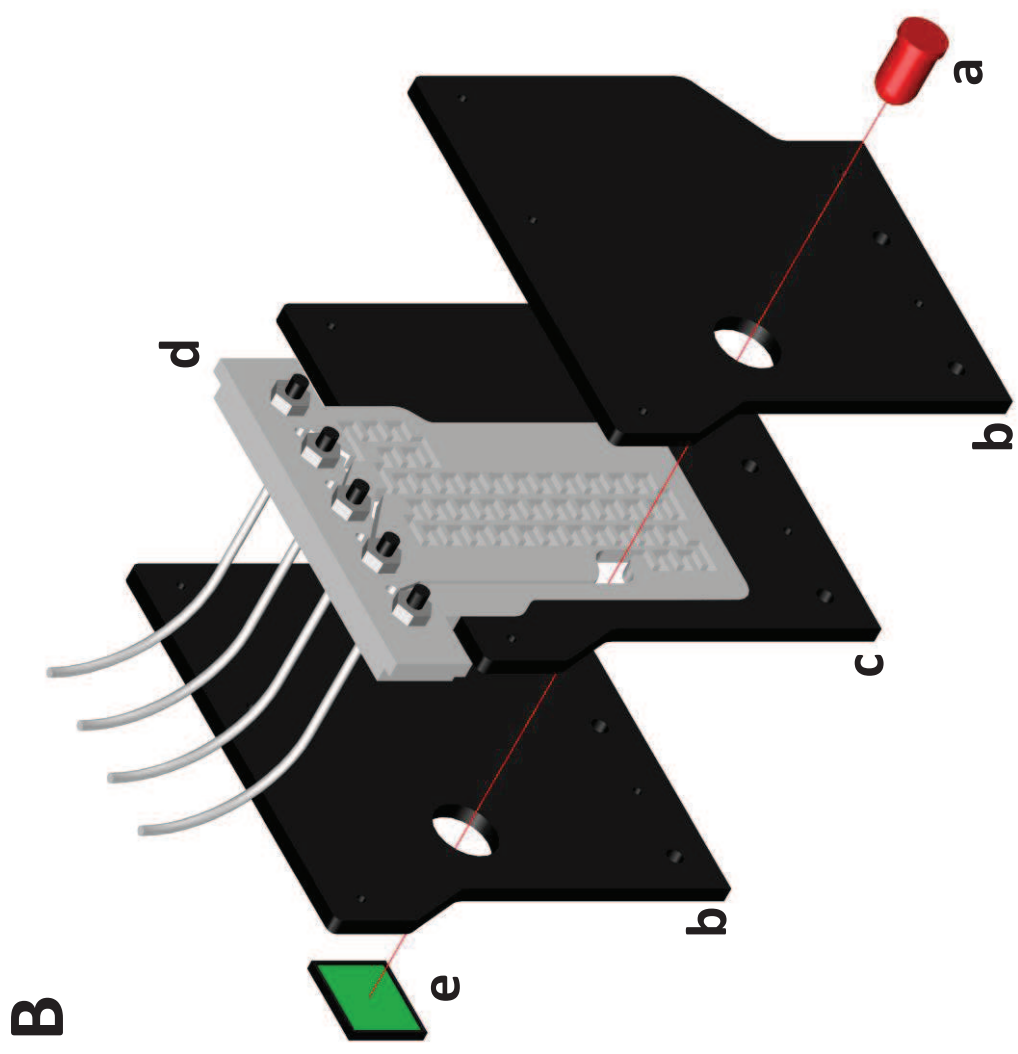
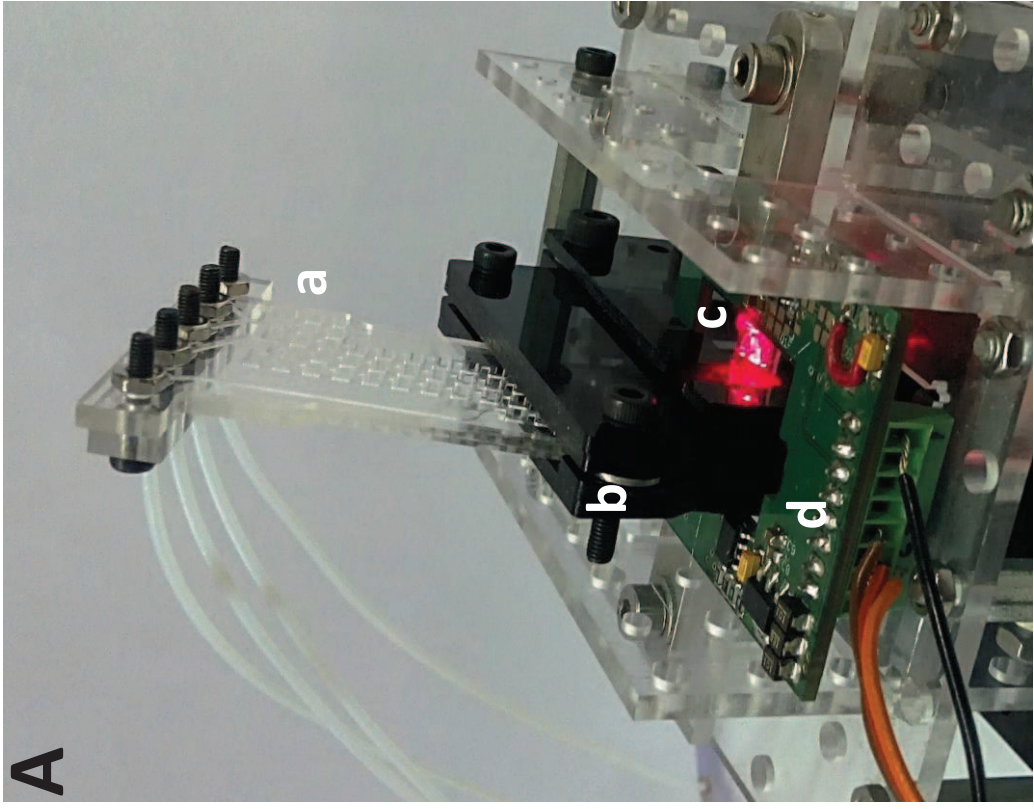


Figure 3

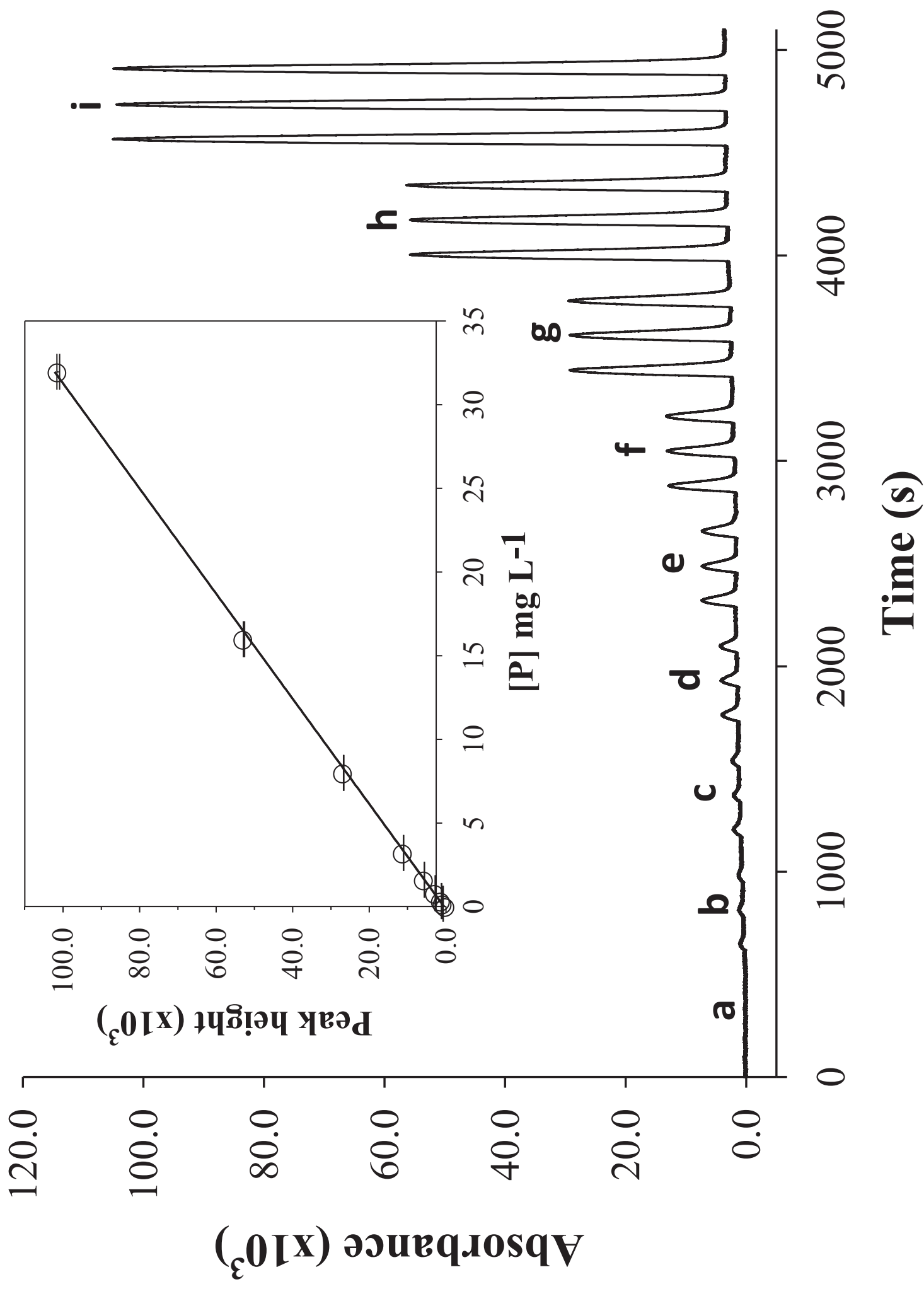


Figure 4

**Figure 1. A:** Design of the prototype layers. Layers “a” and “b” are Topas plaques of 1mm, layer “c” is a Topas plaque of 500  $\mu\text{m}$  thick. Layers “a” and “c” have a Topas foil of 25  $\mu\text{m}$  previously laminated before their machining; **B:** Picture of the final device: **a)** Fluidic connections; **b)** Microfluidics; **c)** Flow-cell.

**Figure 2:** Schematic diagram of the experimental set-up including flow management system, microfluidics and optical detection system where: **a)** reducing solution of 60 mM ascorbic acid; **b)** complexing solution of 5 mM ammonium molybdate in 0.1 M  $\text{H}_2\text{SO}_4$ ; **c)** sample; **d)**  $\text{H}_2\text{O}$ ; **e)** stock solution; **W:** waste outlet; **V<sub>x</sub>:** three-way solenoid microvalve; **PP:** peristaltic micropump; **SP<sub>x</sub>:** solenoid micropump; **C:** controller for fluidic devices; **D:** data acquisition card; **1)** LED at 660 nm; **2)** detection flow-cell; **3)** PIN-photodiode. Solid lines are fluidic connections and dotted lines are electric connections

**Figure 3. A:** Picture of the microdevice while inserted in the optical detection system: **a)** microanalyzer; **b)** lock-and-key insertion port; **c)** LED at 660 nm; **d)** PCB with the electronics associated to the control and acquisition of the signal. **B:** Scheme of the lock-and-key concept of the optical detection system: **a)** LED at 660 nm; **b)** mask with a circular hole that only allows light to pass through the flow-cell; **c)** layer acting as lock of the insertion port; **d)** microanalyzer acting as key; **e)** PIN-photodiode.

**Figure 4.** Signal recording and calibration curve for the microanalyzer using a multicommutation dilution program from a stock solution of  $\text{NaH}_2\text{PO}_4$  of 32  $\text{mg L}^{-1}$  P per triplicate. Obtained standard solutions were of 0  $\text{mg L}^{-1}$  (**a**), 0.16  $\text{mg L}^{-1}$  (**b**), 0.32  $\text{mg L}^{-1}$  (**c**), 0.80  $\text{mg L}^{-1}$  (**d**), 1.60  $\text{mg L}^{-1}$  (**e**), 3.20  $\text{mg L}^{-1}$  (**f**), 8.00  $\text{mg L}^{-1}$  (**g**), 16.00  $\text{mg L}^{-1}$  (**h**) and 32.00  $\text{mg L}^{-1}$  (**i**).